Electronic Structure and Bonding in Four-Coordinate Organometallic Complexes of Aluminum. Valence Photoelectron Spectra of BHT-H, $Me_3Al(PMe_3)$, and $Me_2(BHT)Al(PMe_3)$

Dennis L. Lichtenberger,*,† Royston H. Hogan,† Matthew D. Healy,‡ and Andrew R. Barron*,‡

Contribution from the Laboratory for Electron Spectroscopy and Surface Analysis, Department of Chemistry, University of Arizona, Tucson, Arizona 85721, and Department of Chemistry, Harvard University, Cambridge, Massachusetts 02138. *Received September 13, 1989*

Abstract: The He I valence photoelectron spectra of the Lewis acid-base adducts $Me_3Al(PMe_3)$ and $Me_2(BHT)Al(PMe_3)$ (BHT-H = 2,6-di-*tert*-butyl-4-methylphenol) have been obtained to characterize the electronic structure and bonding in four-coordinate organometallic complexes of aluminum. To aid in the assignment of the spectrum of $Me_2(BHT)Al(PMe_3)$, the spectrum of the free alcohol, BHT-H, was also obtained. The first and second ionizations of the free BHT-H alcohol show vibrational progressions associated with the symmetric C-C phenyl ring stretching modes, consistent with the b_1 and a_2 π ionizations, respectively, of monosubstituted phenyl rings. In the photoelectron spectrum of BHT coordinated to aluminum in $Me_2(BHT)Al(PMe_3)$, the corresponding phenoxide a_2 ionization retains the vibrational structure, but the individual vibrational components are lost in the ionization that corresponds most closely with the b_1. The loss of vibrational fine structure associated with ionization from the phenyl π b_1 orbital in the coordinated phenoxide shows that the phenoxide is involved in a π interaction with the $Me_2Al(PMe_3)$ portion of the molecule. In addition, the aluminum center in $Me_2(BHT)Al(PMe_3)$ feels a more negative charge potential than the aluminum center in $Me_3Al(PMe_3)$, as shown by the Al-P σ ionization occurring at lower binding energy in $Me_2(BHT)Al(PMe_3)$. This is counter to the σ inductive effects of an alkoxide compared to an alkyl and shows that the BHT is acting as a π electron donor. The change in band shape of the Al-P σ ionization between $Me_3Al(PMe_3)$ and $Me_2(BHT)Al(PMe_3)$ indicates that the oxygen p π orbital of the phenoxide ligand is interacting directly with the Al-P bonding orbital. The relationship between experimental ionization potentials and bond strengths of the Al-P σ bond in $Me_3Al(PMe_3)$ and $Me_2(BHT)Al(PMe_3)$ is developed, and the results show that the Al-P σ bond is stronger in $Me_3Al(PMe_3)$ than in $Me_2(BHT)Al(PMe_3)$, consistent with π donation from the phenoxide into the predominantly Al-P σ^* orbital.

Lewis acid-base adducts are a common occurrence in both main-group and transition-metal chemistry. Many transition-metal complexes may be conceptualized as Lewis acid-base adducts arising from the interaction between a two-electron donor ligand (the Lewis base) and a coordinatively unsaturated metal fragment (the Lewis acid). The widespread occurrence of such Lewis acid-base adducts has prompted a number of theoretical and experimental studies into the electronic structure and bonding characteristics of this class of compounds.[1-5] Among the main-group metals, the Lewis acid-base chemistry of the elements of the boron, aluminum, and gallium group is particularly varied and extensive.[6] The bonding modes in these molecules provide important comparisons and contrasts with the transition-metal systems.

We have recently reported the synthesis and structural characterization of Lewis acid-base adducts of aluminum containing the sterically hindered aryl oxide 2,6-di-*tert*-butyl-4-methoxyphenol (BHT-H, from the trivial name butylated hydroxytoluene).[7] These complexes may be conveniently described as Lewis acid-base adducts in which the Lewis acid is a three-coordinate aluminum fragment, such as $Me_2(BHT)Al$ or $Me(BHT)_2Al$, and the base is a phosphine ligand, typically trimethylphosphine. These adducts show a number of interesting features. For example, the Al-O-C angle [164.5 (4)°] in one of the compounds, $Me_2(BHT)Al(PMe_3)$, is much larger than previously observed in main-group alkoxides.[7] In addition, the Al-O distance [1.736 (5) Å] is short compared to the normal range of 1.8-2.0 Å. The shortening of the Al-O bond length, along with the increase in the Al-O-C angle, suggests the presence of an additional bonding interaction, possibly of the π type between the oxygen and four-coordinate aluminum center. The π-donor abilities of alkoxides to transition metals have been discussed extensively in terms of the availability of empty metal d orbitals on the transition-metal centers.[8,9] However, d orbitals on aluminum are not similarly accessible. The exact nature of the interaction between the alkoxide and the aluminum center is, therefore, of special interest.

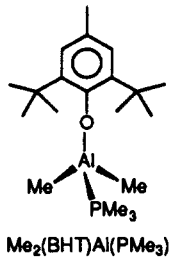

$Me_2(BHT)Al(PMe_3)$

Photoelectron spectroscopy provides a direct experimental probe of the bonding characteristics and electron distribution within a molecule.[10-12] The technique has been used extensively to experimentally probe the nature of the dative bond in Lewis acid-base adducts. This paper describes the valence ionizations of $Me_3Al(PMe_3)$ and $Me_2(BHT)Al(PMe_3)$. The valence photoelectron spectrum of the free alcohol is included as an aid in the assignment of the ionizations. Particular emphasis is placed on the observation of vibrational fine structure in the spectral features.

* To whom correspondence should be addressed.
† University of Arizona.
‡ Harvard University.

(1) Mihai, E.; Hoffmann, R. *Inorg. Chem.* **1975**, *14*, 1058-1076.
(2) Albright, T. A.; Burdett, J. K.; Whangbo, M. H. *Orbital Interactions In Chemistry*; Wiley: New York, 1985.
(3) Bossett, P. J.; Lloyd, D. R. *J. Chem. Soc., Dalton. Trans.* **1972**, 248.
(4) Lloyd, D. R.; Lynaugh, N. *J. Chem. Soc., Faraday Trans. 2* **1972**, 68, 947.
(5) Lake, R. F. *Spectrochim. Acta., Part A* **1971**, *27A*, 1220.
(6) *Comprehensive Organometallic Chemistry*; Wilkinson, G., Stone, F. G. A., Abel, E. W., Eds.; Pergamon: New York, 1982; Vol. 1, Chapters 5-7.
(7) Healy, M. D.; Wierda, D. A.; Barron, A. R. *Organometallics* **1988**, *7*, 2543.
(8) Chisholm, M. H. *Polyhedron* **1983**, *2*, 681.
(9) Coffindaffer, T. W.; Steffy, B. D.; Rothwell, I. P.; Folting, K.; Huffman, J. C.; Streib, W. E. *J. Am. Chem. Soc.* **1989**, *111*, 4742.
(10) Lichtenberger, D. L.; Kellogg, G. E. *Accts. Chem. Res.* **1987**, *20*, 379.
(11) Lichtenberger, D. L.; Kellogg, G. E.; Pang, L. S. K. In *New Developments in the Synthesis, Manipulation and Characterization of Organometallic Compounds*; Wayda, A. L., Darensbourg, M. Y., Eds.; ACS Symposium Series; American Chemical Society: Washington, DC, 1989; 357.
(12) Lichtenberger, D. L.; Kellogg, G. E. *Modern Inorganic Chemistry*; Fackler, J. P., Ed.; 1989.

0002-7863/90/1512-3369$02.50/0

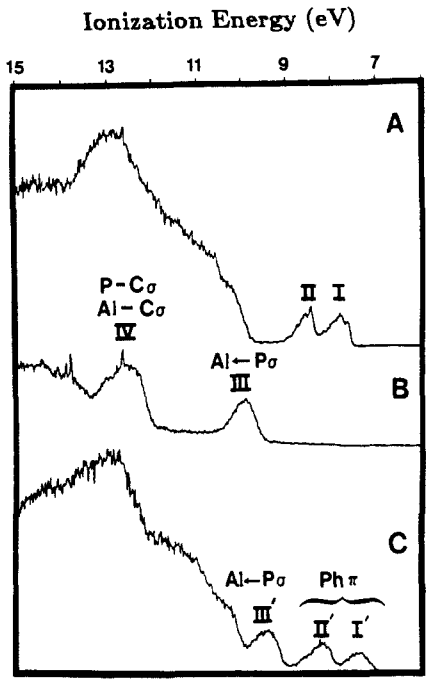

Figure 1. Full He I photoelectron spectrum of BHT-H (A), $Me_3Al(PMe_3)$ (B), and $Me_2(BHT)Al(PMe_3)$ (C).

The shifts in ionization energies between related compounds also contribute to the evaluation of the σ and π contributions to the Al-O bond and the factors influencing the strength of the Al-PMe_3 bonds.

Experimental Section

$Me_3Al(PMe_3)$ and $Me_2(BHT)Al(PMe_3)$ were prepared by previously reported methods.[7] BHT-H was obtained from Aldrich and sublimed prior to use. Photoelectron spectra were recorded on an instrument that features a 36-cm-radius hemispherical analyzer (10-cm gap) and customized sample cells, excitation sources, detection and control electronics, and data collection methods that have been described previously.[13-16] He I data were collected at sample cell temperatures of 25, 18, and 75 °C for BHT-H, $Me_3Al(PMe_3)$, and $Me_2(BHT)Al(PMe_3)$, respectively. All samples sublimed cleanly. The data are represented analytically with the best fit of asymmetric Gaussian peaks (program GFIT).[17,18] The asymmetric Gaussian peaks are defined by the peak position, the amplitude, the half-width indicated by the high binding energy side of the peak (W_H), and the half-width indicated by the low binding energy side of the peak (W_L). The confidence limits of the peak positions and widths are generally ±0.02 eV. The observed fine structure in a band is modeled with a progression of component peaks that are constrained to be equally spaced and have the same shapes. The number of peaks and the spacing between them are optimized to model the band contour. These constraints held to a minimum the number of independently varying parameters required to model the vibrational progression.[18]

Results

Valence Ionization Bands and Assignments. The He I valence photoelectron spectra of $Me_3Al(PMe_3)$ and $Me_2(BHT)Al(PMe_3)$ are shown in Figure 1. The assignment of the spectrum of $Me_2(BHT)Al(PMe_3)$ is aided by comparison to the spectrum of the BHT-H molecule, which is also included in Figure 1. The spectra of BHT-H and the corresponding aluminum molecule show a broad band of overlapping ionizations from about 9.5-15.5 eV. This forest of ionizations is due to C-H and C-C valence σ ionizations and oxygen lone-pair ionizations. Individual assignments in this region will not be attempted.

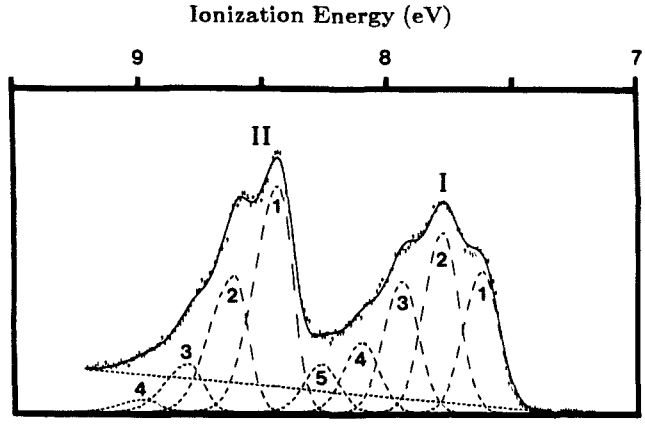

Figure 2. Close-up He I spectrum of BHT-H.

Chart I

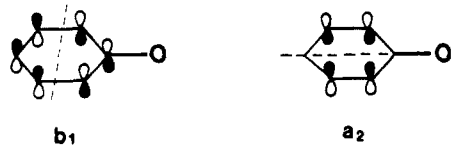

Table I. He I Valence Ionization Features of BHT-H (BHT = 2,6-Di-*tert*-butyl-4-methylphenoxide)

band		posn	W_H	W_L	rel area		
I	1	7.62	0.17	0.16	1.00		
	2	7.78	0.17	0.16	1.27		
	3	7.94	0.17	0.16	0.93		
	4	8.09	0.17	0.16	0.17	0.16	0.50
	5	8.26	0.17	0.16	0.34		
II	1	8.43	0.23	0.13	1.76		
	2	8.61	0.23	0.13	1.05		
	3	8.79	0.23	0.13	0.37		
	4	8.97	0.23	0.13	0.10		

A close-up spectrum of the ionizations of BHT-H in the 6-9-eV region is shown in Figure 2. On the basis of previous studies of the leading ionizations of phenol and its substituted derivatives,[19,20] bands I and II in Figure 2 are assigned to ionizations associated with two of the π-system orbitals of the phenyl ring. The nodal characteristics of these orbitals in relation to the oxygen atom on the ring are illustrated in Chart I. In monosubstituted phenyl compounds with C_{2v} symmetry, these orbitals are the b_1 and a_2 symmetry combinations, respectively, of the phenyl ring carbon p π orbitals. The a_2 orbital has a node at the carbon that is bound to the oxygen atom, while the b_1 orbital has a substantial contribution from this carbon atom. The interaction of the b_1 symmetry combination with a filled p π orbital on the oxygen atom destabilizes the resulting b_1 ionization relative to the a_2 ionization. Although the molecular symmetry of BHT-H is C_s and the true orbital symmetries of the Phπ orbitals are both a'', the same basic nodal characteristics and atomic orbital interactions are taking place in the π framework. The b_1 and a_2 labels will be retained when referring to these orbitals. In the photoelectron spectrum of BHT-H, bands I and II are assigned to ionizations associated with the b_1 and a_2 orbitals, respectively.

The contours of both ionization bands show the presence of vibrational progressions. Band I is modeled by five asymmetric Gaussian peaks spaced 0.16 eV (±0.01 eV) apart. The contour of band II is represented by four asymmetric Gaussian components with a spacing of 0.18 eV (±0.01 eV). The vertical and adiabatic

(13) Kellogg, G. E. *Diss. Abstr. Int. B* **1986**, *46*, 3838.
(14) Calabro, D. C.; Hubbard, J. L.; Blevins, C. H., II; Campbell, A. C.; Lichtenberger, D. L. *J. Am. Chem. Soc.* **1981**, *103*, 6739.
(15) Lichtenberger, D. L.; Kellogg, G. E.; Kristofzski, J. G.; Page, D.; Turner, S.; Klinger, G.; Lorenson, J. *Rev. Sci. Instrum.* **1986**, *57*, 2366.
(16) Hubbard, J. L. *Diss. Abstr. Int. B* **1983**, *43*, 2203.
(17) Lichtenberger, D. L.; Fenske, R. F. *J. Am. Chem. Soc.* **1976**, *98*, 50.
(18) Copenhaver, A. S. Ph.D. Dissertation, University of Arizona, 1989.
(19) Kimura, K.; Katsumata, S.; Achiba, Y.; Iwata, S.; Yamazaki, T. *Handbook of He(I) Photoelectron Spectra of Fundamental Organic Molecules*; Halsted Press: New York, 1980.
(20) Turner, D. W.; Baker, C.; Baker, A. D.; Brundle, C. R. *Molecular Photoelectron Spectroscopy. A Handbook of He 584 Å Spectra*; Wiley-Interscience: New York.

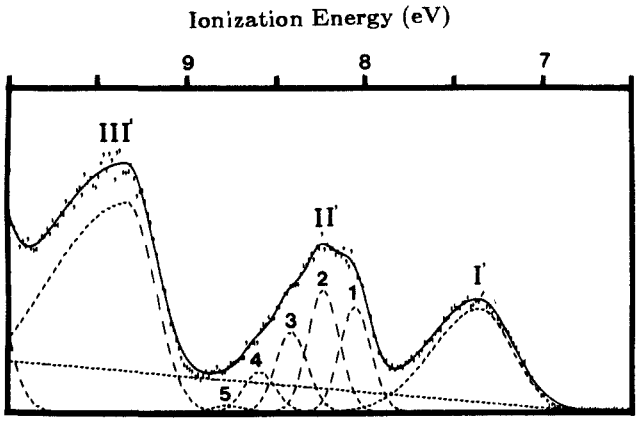

Figure 3. Close-up HeI spectrum of $Me_2(BHT)Al(PMe_3)$.

IP's of these bands are listed in Table I. The spacings between the Gaussian components correspond to vibrational frequencies in the ranges 1200–1400 cm^{-1} for band I and 1350–1550 cm^{-1} for band II. In-plane C–H bending in phenyl compounds appears in the range 1000–1300 cm^{-1} while skeletal vibrations involving carbon to carbon stretching within the ring fall in the 1400–1500- and 1585–1600-cm^{-1} regions.[21] Of these two modes, ionization from the Ph π orbitals has a greater effect on the carbon–carbon bond order and will activate the C–C skeletal mode to a larger extent than the in-plane bending mode. Vibrational fine structure has occasionally been observed in the b_1 and a_2 ionizations of other monosubstituted benzene molecules.[22] In molecules with simple substitutions two vibrational modes may be observed, one in the range 1540–1690 cm^{-1} that is similarly assigned to the symmetric C–C stretching mode and one in the range of 520–560 cm^{-1} depending on the heteroatom bound to the benzene ring. We do not independently observe the lower frequency vibrational progression, although it may contribute to deviations of the fit from the band contour in Figure 2 and influence the frequency we obtain. The important point for this study is that ionizations from the b_1 and a_2 orbitals in the neutral ground state of the molecule give rise to vibrational progressions from C–C bond stretching of the phenyl ring of the positive ion.

The photoelectron spectrum of $Me_3Al(PMe_3)$ (see Figure 1) displays two broad features at 9.87 and ≈12.5 eV. These will be referred to as band III and band IV, respectively, to avoid confusion with the ionizations of BHT–H. Band III is assigned to ionization from the Al–P σ-bonding orbital, which is formed primarily from donation of the phosphorus lone pair to the Al^{III} center. This assignment follows from comparison with the spectrum of free PMe_3 and other metal–PMe_3 species.[13,23,24] The ionization energy of the phosphorus lone pair in free PMe_3 is 8.58 eV,[25] so the position of band III corresponds to a stabilization of 1.29 eV for the phosphorus lone pair upon coordination to aluminum in this molecule. Very similar values of 1.32 and 1.29 eV, respectively, are seen for stabilization of the phosphorus lone pair on coordination to the transition-metal complexes such as $(CO)_5Mo(PMe_3)$ and $CpMn(CO)_2(PMe_3)$.[13,23,24] Band IV is assigned to ionizations associated with the "e" sets of the P–C σ bonds of the PMe_3 ligand and the Al–Me σ bonds of $Me_3Al(PMe_3)$. The ionization energy of the "e" set of P–C σ bonds in PMe_3 occurs at 11.31 eV, and hence a stabilizing shift of ≈0.7–1.0 eV is observed for these ionizations of the complex compared to the corresponding ionizations of the free PMe_3 ligand.

Table II. He I Valence Ionization Features of $Me_2(BHT)Al(PMe_3)$ and $Me_3Al(PMe_3)$

band		posn	W_H	W_L	rel area
		$Me_2(BHT)Al(PMe_3)$			
I'		7.36	0.63	0.43	1.00
II'	1	8.06	0.20	0.22	0.40
	2	8.24	0.20	0.22	0.47
	3	8.42	0.20	0.22	0.31
	4	8.60	0.20	0.22	0.15
	5	8.78	0.20	0.22	0.02
III'		9.34	1.09	0.35	2.78
		$Me_3Al(PMe_3)$			
III		9.87	0.73	0.43	1.0

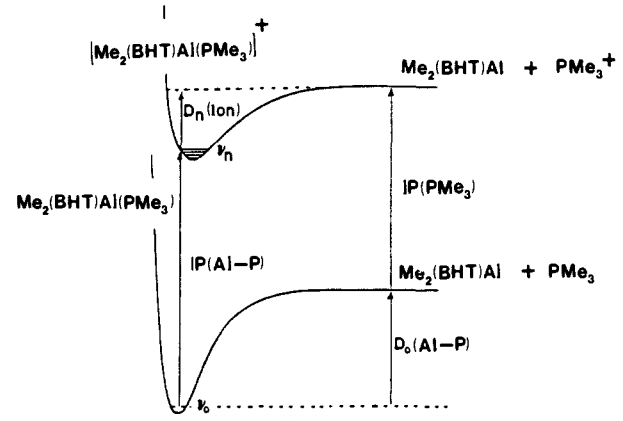

Figure 4. Relationship between the ionization energies and potential wells of $Me_2(BHT)Al(PMe_3)$ and the corresponding $Me_2(BHT)Al$ and PMe_3 molecules.

A close-up photoelectron spectrum of $Me_2(BHT)Al(PMe_3)$ is shown in Figure 3. The first two ionizations correlate with ionizations from the b_1 and a_2 phenyl π orbitals of the phenoxide ligand and are labeled bands I' and II', respectively. Band I' lacks resolvable fine structure and is best represented by a single broad asymmetric Gaussian peak. The profile of this ionization is important to the interpretation of the electronic interactions in this molecule. Band II' shows a vibrational progression that is represented by five nearly symmetric Gaussian peaks spaced 0.18 ± 0.01 eV apart. This is the same vibrational frequency observed for the corresponding ionization of BHT–H, and it is similarly assigned to C–C stretching of the phenyl ring.

Band III', with a vertical IP of 9.3 eV in the spectrum of $Me_2(BHT)Al(PMe_3)$, is assigned to ionization from the Al–P σ-bonding orbital. This ionization correlates with the similar ionization (band III in Figure 1) in the spectrum of $Me_3Al(PMe_3)$, but it occurs at 0.6 eV lower binding energy. Band III' is best fit by a single asymmetric Gaussian peak that is skewed to the higher binding energy side of the band.

Discussion

Comparison of the coordinated phosphorus lone-pair ionizations between $Me_3Al(PMe_3)$ and $Me_2(BHT)Al(PMe_3)$ shows that the interaction between the BHT ligand and the aluminum center must involve more than traditional σ bonding. On the basis of the lower group electronegativity of the methyl ligand compared to a phenoxide ligand,[26] the aluminum center in the trimethyl compound should be more electron rich, and this in turn would destabilize the ionization of the phosphine lone pair coordinated to Me_3Al relative to $Me_2(BHT)Al$. However, exactly the opposite is observed. The phosphorus lone pair in $Me_3Al(PMe_3)$ is shifted 0.53 eV to higher binding energy than the corresponding ionization in $Me_2(BHT)Al(PMe_3)$. The shapes and structures of the individual ionizations, as well as the relative shifts, are particularly

(21) Silverstein, R. M.; Bassler, G. C.; Morrill, T. C. *Spectrometric Identification of Organic Compounds*, 4th ed.; Wiley and Sons: New York, 1980.
(22) Dedies, T. P.; Rabalais, J. W. *J. Electron Spectrosc. Relat. Phenom.* **1972**, *1*, 355–70.
(23) Bursten, B. E.; Darensbourg, D. J.; Kellogg, G. E.; Lichtenberger, D. L. *Inorg. Chem.* **1984**, *23*, 4361.
(24) Bancroft, G. M.; Dignard-Bailey, L.; Puddephatt, R. J. *Inorg. Chem.* **1986**, *25*, 3675.
(25) Hillier, I. H.; Saunders, U. R. *J. Chem. Soc., Faraday Trans.* **1970**, 2401.
(26) Bromilow, J.; Brownlee, R. T. C.; Lopez, V. O.; Taft, R. W. *J. Org. Chem.* **1979**, *44*, 4766.

interesting. The discussion that follows shows that these ionizations provide an array of chemically relevant information, such as the relative strength of the Al–P bonds in these complexes and the ligating characteristics of the phenoxide ligand.

Comparison of the Al–P Bond Strengths. On the basis of the ionization information obtained from the aluminum complexes and the free PMe_3 ligand, a qualitative comparison of the Al–P σ bond dissociation energies in $Me_3Al(PMe_3)$ and $Me_2(BHT)Al(PMe_3)$ is readly available. The underlying theory has been developed elsewhere[18,27,28] and will be reviewed here very briefly for the case of $Me_3Al(PMe_3)$ and $Me_2(BHT)Al(PMe_3)$. The relationship between the Al–P σ bond dissociation energies in $Me_3Al(PMe_3)$ and $Me_2(BHT)Al(PMe_3)$ and the ionization potential of this bond in these two molecules are illustrated in Figure 4. D_0(Al–P) is the dissociation energy of the Al–P bond for the neutral $Me_3Al(PMe_3)$ and $Me_2(BHT)Al(PMe_3)$ molecules. IP(Al–P) is the measured ionization potential from the predominantly Al–P σ orbital of the neutral molecule to a final ion state. $IP(PMe_3)$ is the measured ionization potential of the phosphorus lone pair of the free PMe_3 molecule, and D_n(ion) is the Al–P bond dissociation energy from the appropriate vibrational state of the molecular ions of $Me_3Al(PMe_3)$ or $Me_2(BHT)Al(PMe_3)$. Figure 4 uses the vibrational state corresponding to the vertical ionization energy. The individual energy contributions to the energy cycle illustrated in Figure 4 gives the equation

$$D_0(\text{Al–P}) = D_n(\text{ion}) + \text{IP(Al–P)} - \text{IP}(PMe_3) \quad (1)$$

The Al–P bond dissociation energy in the molecular ion is a proportion (λ) of the Al–P dissociation energy of the neutral molecule:

$$\lambda D_0(\text{Al–P}) = D_n(\text{ion}) \quad (2)$$

Removal of an electron from a completely covalent bond reduces the bond order by half, and $\lambda \approx 0.5$. Oxidation of the complex also contributes to bond weakening in organometallic molecules, and λ (fraction of bond energy left in the positive ion) can tend toward zero. Most bonds may be considered to be somewhere between these two extremes. In general, $0.5 \geq \lambda \geq 0$.

Subtituting (1) into (2) gives the following equation:

$$(1 - \lambda)D_0(\text{Al–P}) = \text{IP(Al–P)} - \text{IP}(PMe_3) \quad (3)$$

Assuming that λ is approximately the same in $Me_3Al(PMe_3)$ and $Me_2(BHT)Al(PMe_3)$, the ratio of the Al–P bond strengths in $Me_3Al(PMe_3)$ and $Me_2(BHT)Al(PMe_3)$ is given by the ratio of the ionization energy stabilization of the phosphorus lone pair with coordination to aluminum:

$$\frac{D_0(\text{Al–P})[Me_3Al(PMe_3)]}{D_0(\text{Al–P})[Me_2(BHT)Al(PMe_3)]} = \frac{\text{IP(Al–P)}/Me_3Al(PMe_3) - \text{IP}(PMe_3)}{\text{IP(Al–P)}/Me_2(BHT)Al(PMe_3) - \text{IP}(PMe_3)} \quad (4)$$

Substituting the ionization potentials obtained from this study gives a value of ≈ 1.6 for the ratio of the Al–P bond dissociation energies of $Me_3Al(PMe_3)$ and $Me_2(BHT)Al(PMe_3)$. This indicates that the Al–P σ bond is considerably stronger in $Me_3Al(PMe_3)$ than in $Me_2(BHT)Al(PMe_3)$. The reason for the stronger Al–P σ bond in $Me_3Al(PMe_3)$ is addressed in the following sections, where we discuss the experimental evidence for phenoxide π donation.

Photoelectron Observations of π Donation from BHT to $Me_2Al(PMe_3)$. The changes in vibrational fine structure of the phenyl π ionizations between the free and coordinated phenoxide ligand show that the phenoxide ligand has a significant π interaction with the $Me_2Al(PMe_3)$ portion of the molecule. In the photoelectron spectrum of the free phenol, both the b_1 (first ionization) and the a_2 (second ionization) show vibrational progressions associated with the C–C skeletal stretching of the phenyl ring. In the coordinated phenoxide ligand the corresponding a_2 ionization retains the vibrational fine structure that is observed in the spectrum of the free ligand. However, the fine structure associated with the b_1 ionization in the free ligand is replaced in the coordinated phenoxide by a broad asymmetric Gaussian peak. The obscuring of the vibrational fine structure in the b_1 ionization with coordination is due to access to additional closely spaced vibrationally excited positive-ion states. This means that the b_1 becomes significantly more delocalized with coordination to $Me_2Al(PMe_3)$ while the localization of the a_2 does not significantly change. The b_1 orbital has a π-symmetry interaction with the aluminum center in the plane of the Al–P bond (vide infra). The additional vibrationally excited positive-ion states with b_1 ionization arise from vibrational modes associated with the $Me_2Al(PMe_3)$ moiety.

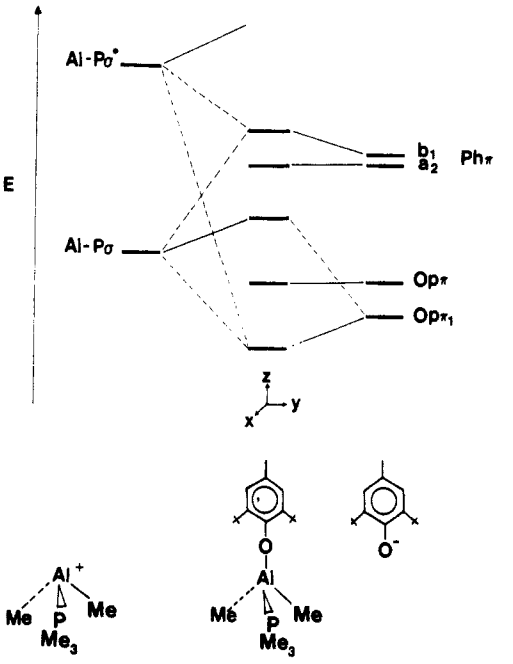

Figure 5. Ionization correlation diagram showing the interactions between the frontier orbitals of BHT and $[Me_2Al(PMe_3)]^+$.

An additional indication of the phenoxide π interaction is provided by the Al–P σ ionizations. The band shape associated with the Al–P σ ionization differs considerably between $Me_3Al(PMe_3)$ and $Me_2(BHT)Al(PMe_3)$. The band is considerably broader in the latter complex and skewed to the high binding enery side, indicating that the ionization from the Al–P σ orbital in $Me_2(BHT)Al(PMe_3)$ gives rise to a larger number of vibrationally excited positive-ion states compared to the corresponding ionization in $Me_3Al(PMe_3)$. Because the difference in ligand environment between the two complexes lies in the replacement of a methyl group in $Me_3Al(PMe_3)$ by a phenoxide ligand, the observed increase in vibrational states of the positive ion associated with the Al–P σ ionization in $Me_2(BHT)Al(PMe_3)$ compared to $Me_3Al(PMe_3)$ is due to vibrations associated with the phenoxide ligand.

When the overall charge potential at the Al center is compared in $Me_2(BHT)Al(PMe_3)$ and $Me_3Al(PMe_3)$, the better π-donor ability of the phenoxide compared to methyl is countered by the poorer σ-donor ability of the more electronegative phenoxide. The $Me_2Al(PMe_3)$ portion of the molecule must also have an available empty orbital to accept the π-electron charge from the BHT. The net change in charge potential depends on which of the σ or π factors dominate. A destabilization of 0.53 eV is observed for the phosphorus lone-pair ionization in $Me_2(BHT)Al(PMe_3)$ compared to $Me_3Al(PMe_3)$, indicating a more negative charge potential at the Al center in $Me_2(BHT)Al(PMe_3)$ than in $Me_3Al(PMe_3)$. The magnitude of phenoxide π donation into an available orbital on $Me_2Al(PMe_3)$ is hence greater than the

(27) Lichtenberger, D. L.; Darsey, G. P.; Kellogg, G. E.; Sanner, R. D.; Young, V. G. *J. Am. Chem. Soc.* **1989**, *111*, 5019.
(28) Lichtenberger, D. L.; Copenhaver, A. S. *Thermodynamics of Organometallic Compounds*; Marks, T., Ed.; ACS Symposia-In-Print; American Chemical Society: Washington, DC, submitted for publication.

Chart II

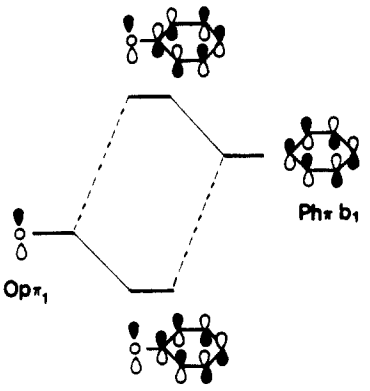

difference in σ-donating abilities of the phenoxide and the methyl ligands.

Ionization Correlation Diagram. The interactions between the frontier orbitals of the BHT ligand and $Me_2Al(PMe_3)$ indicated by the photoelectron data are illustrated in Figure 5. The central column in Figure 5 shows the ionization energies of $Me_2(BHT)Al(PMe_3)$. The relative positions of the occupied frontier orbitals of the BHT and $Me_2Al(PMe_3)$ fragments in the molecule are estimated from the ionization energies of the parent molecules. BHT-H and $Me_3Al(PMe_3)$ as specified below.

The frontier orbitals of BHT on the right of Figure 5 are labeled according to their primary character, but it should be remembered that the predominantly phenyl π b_1 orbital includes mixing with an oxygen p π orbital. The interactions between the oxygen lone pair and Ph π b_1 orbitals are illustrated in Chart II. The orbitals are the correct symmetry to form filled bonding and antibonding π combinations between the oxygen atom and the ring. The bonding combination is predominantly oxygen lone pair in character and is labeled O p π_1 in Figure 5, while the antibonding combination is largely the Ph π b_1. The orbital labeled O p π in Figure 5 is in the plane of the phenyl ring and does not overlap with the phenyl π orbitals.

The Al-P σ ionization on the left of Figure 5 is positioned at the ionization energy observed for $Me_3Al(PMe_3)$. The most pertinent interactions involve the predominantly Al-P σ and σ^* orbitals, and therefore the virtual Al-P σ^* orbital is included in the diagram. For clarity, the Al-Me σ bonds are not included in the diagram because of the relative stability of the Al-Me σ bonds observed in the PES of $Me_3Al(PMe_3)$. Similarly, the Al-Me σ^* orbitals are expected to be higher in energy than the Al-P σ^* orbital and interact less strongly with the phenoxide. In support of these expectations, the crystallographic study of $Me_2(BHT)Al(PMe_3)$[7] shows that the phenoxide ligand is rotated so that the O p π_1 and Ph π b_1 orbitals have optimum interaction with the Al-P σ and σ^* orbitals (see Figure 5). Furthermore, the phenoxide ligand displays a distinct tilt toward the Al-P bond [O-Al-P = 104.5 (2)°].

When the frontier orbital overlap interactions between BHT and $Me_2Al(PMe_3)$ are considered, it is first recognized that the Al-P σ and σ^* orbitals lie on the nodes of the phenoxide a_2 ring orbital and the O p π orbital (which is in the plane of the phenyl ring). The energies of the Ph π a_2 and O p π are not influenced by overlap with the Al-P orbitals, and therefore these ionization energies of $Me_2(BHT)AlPMe_3$ are drawn parallel to the corresponding ionizations of BHT-H, with the other ionizations of BHT-H adjusted accordingly to the potential field of BHT in the molecule.

The O p π_1 and Ph π b_1 orbitals have the correct symmetry to interact with the filled Al-P σ-bonding orbital (localized on phosphorus) and with the unfilled Al-P σ^* orbital (which is largely Al p π in character). The interactions of the Al-P σ bond with the filled orbitals on the phenoxide have a slightly destabilizing influence on the complex since these are filled-filled interactions. These filled-filled interactions also do not result in any net electron transfer from the phenoxide to the aluminum portion of the molecule. The energy effect of these interactions is observed primarily in the additional destabilization of the b_1 ionization relative to the a_2. The separation between the vertical b_1 and a_2 ionizations of the free BHT-H molecule is 0.65 eV, and the separation of the corresponding ionizations of the coordinated phenoxide is 0.88 eV. The additional vibrational modes in the predominantly Ph π b_1 ionization of the $Me_2(BHT)Al(PMe_3)$ molecule, which obscure the simple C-C ring stretching progression, follow from this mixing.

Table III. Ionization Potentials of the Phosphorus Lone Pair in $Me_2(BHT)Al(PMe_3)$, and Some Transition-Metal Complexes

compound	IP (eV)
PMe_3[a]	8.58
$Me_2(BHT)Al(PMe_3)$	9.34
$Me_3Al(PMe_3)$	9.87
$CpMn(CO)_2PMe_3$[a]	9.87
$(CO)_5Mo(PMe_3)$[a]	9.90
cis-$(CO)_4Mo(PMe_3)_2$[a]	9.53, 9.56
trans-$(CO)_4Mo(PMe_3)_2$[a]	8.92, 10.22
fac-$(CO)_3Mo(PMe_3)_3$[a]	9.06, 9.44

[a] Reference 13.

The primary mechanism for the transfer of electron density from the oxygen atom to the aluminum center is through interaction of the filled O p π_1 and Ph π b_1 orbitals with the unfilled Al-P σ^* orbital. The donation to the antibonding Al-P σ^* orbital also weakens the net Al-P bond energy in the $Me_2(BHT)Al(PMe_3)$ molecule compared to the $Me_3Al(PMe_3)$ molecule. The extra electron density at the aluminum center and the weaker Al-P bond in the phenoxide complex compared to the trimethyl complex are observed in the lower ionization energy of the Al-P σ ionization. The formal relationship between the ionization energies and the relative bond energies was presented earlier. Thus, the strengthening of the BHT bonding to the complex through π donation from the BHT is at the expense of the strength of the aluminum-phosphine bond.

Comparison with Transition-Metal-Phosphine Complexes. The complexes included in this study involve a PMe_3 ligand bound to a coordinatively unsaturated three-coordinate organometallic aluminum complex. The formal oxidation state of the Al center in these species is +3, with no metal electrons indicating an electron-poor system. PMe_3 also binds to transition-metal fragments such as $CpMn(CO)_2$ and $(CO)_5Mo$ in the complexes $CpMn(CO)_2PMe_3$ and $(CO)_5Mo(PMe_3)$. A particularly interesting comparison is that of the charge characteristics of the metal center in the "electron-poor" Al main-group fragments to the "electron-rich" transition-metal fragments $CpMn(CO)_2$ and $(CO)_5Mo$, where the formal oxidation states of the metal centers are +1 and 0, respectively, and each have a formal metal d-electron count of 6.

The ionization potentials of the phosphorus lone pair in $Me_2(BHT)Al(PMe_3)$, $Me_3Al(PMe_3)$, and several transition-metal-PMe_3 complexes are shown in Table III. The ionization potentials of the phosphorus lone pair in the transition-metal complexes lie at slightly higher binding energy than those of the main group. On the basis of formal oxidation states at the metal centers, the PMe_3 ligand would be expected to have higher ionization energies when bound to the main-group fragments. However, the opposite result is observed, indicating that formal oxidation states are not sufficient to account for the observed trends of the ionization potentials of the phosphorus lone pair in the intact complexes. The phosphorus lone-pair ionizations are more dependent on the ligand substitutions on the metal center. A more detailed examination of the ligand environment around the metal centers and the relative metal nuclear core charges of the respective main-group and transition-metal fragments is under way. Further studies, particularly utilizing gas-phase XPS, need to be carried out in order to better understand the overall charge potentials in main-group metal- and transition-metal-phosphine complexes.

Conclusions

This study illustrates the value of photoelectron spectral data in examining a variety of electronic and thermodynamic features associated with four-coordinate organometallic complexes of

aluminum. The relationship between experimentally determined ionization potentials and bond strengths in $Me_3Al(PMe_3)$ and $Me_2(BHT)Al(PMe_3)$ shows that the Al-P σ bond in $Me_3Al(PMe_3)$ is stronger than that in $Me_2(BHT)Al(PMe_3)$. The source of the weaker Al-P σ bond in $Me_2(BHT)Al(PMe_3)$ traces to phenoxide π donation from an oxygen p π orbital into the empty Al-P σ^* orbital. The loss of observable vibrational fine structure in the Ph π b_1 ionization between the free and coordinated ligand and the change in the band shape and position of the Al-P σ ionization between $Me_3Al(PMe_3)$ and $Me_2(BHT)Al(PMe_3)$ provide the evidence of phenoxide π donation. The Al-P σ ionization occurs at higher binding energy in $Me_3Al(PMe_3)$ than in $Me_2(BHT)Al(PMe_3)$, indicating that the positive charge potential of the Al center is greater in $Me_3Al(PMe_3)$. Although π donation into the vacant 3p orbital of a planar, three-coordinate, Al center is expected, the presence of π bonding in four-coordinate Al compounds is a new observation. We are continuing our studies in this area in order to investigate the generality and influence of this interaction on the chemistry of aluminum compounds.

Acknowledgment. D.L.L. acknowledges support by the U.S. Department of Energy (Division of Chemical Sciences, Office of Basic Energy Sciences, Office of Energy Research: Grant DF-SG02-86ER135101), the National Science Foundation (Grant CHE8519560), and the Materials Characterization Program, Department of Chemistry, University of Arizona. A.R.B. acknowledges support by the Petroleum Research Fund administered by the American Chemical Society, and ICI-Materials Division.

An Experimental and Computational Investigation of the Mechanism of the Deoxygenation of THF by Atomic Carbon

Michael L. McKee,* Gitendra C. Paul, and Philip B. Shevlin*

Contribution from the Department of Chemistry, Auburn University, Auburn, Alabama 36849.
Received August 4, 1989

Abstract: An ab initio investigation (MP2/6-31G*//3-21G) of the deoxygenation of tetrahydrofuran (**1**) to ethylene and CO by atomic carbon reveals a low-energy concerted pathway, which yields the products directly in a 3-bond cleavage. The geometry of the transition state for this process, calculated at the HF/3-21G level, indicates a nonsynchronous process in which the C-O bonds are cleaved to a greater extent than the C-C bond. When C atoms are reacted with a 1:1 mixture of **1** and **1**-d_8, the products are ethylene and ethylene-d_4 in a 2.7:1 ratio. This ratio represents a mean secondary kinetic isotope effect (KIE) k_H/k_D = 1.13 per H and is close to a value of 1.12 calculated from the computed amount of rehybridization in the transition state and the corresponding equilibrium isotope effects.

The deoxygenation of tetrahydrofuran (**1**) by atomic carbon,[1] which results in exclusive cleavage to C_2H_4 and CO, is an interesting reaction in that it offers a wide variety of mechanistic possibilities regarding the timing of bond making and breaking (Scheme I).[2] Although it is tempting to postulate the intermediacy of the cisiod tetramethylene biradical **2**, other reactions in which **2** and its derivatives have been generated lead to cyclobutanes as well as ethylenes.[1,3,4] Since no cyclobutanes are generated in the deoxygenation of **1**, it may be that the products in Scheme I result from a concerted 3-bond cleavage of 2 C-O bonds and a C-C bond. In this study, we report an experimental and computational evaluation of the timing of bond breaking in this interesting reaction.

Computational Results. The Gaussian 82[5] and 86[6] programs were used to investigate this reaction theoretically. Geometries

Scheme I

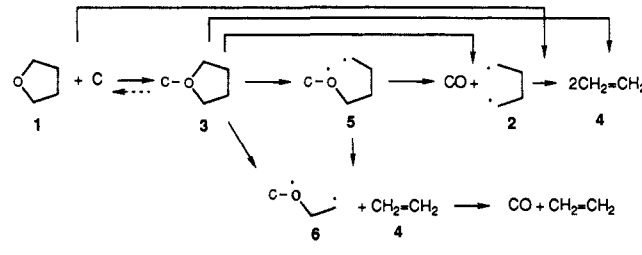

were optimized at the HF/3-21G level, and single-point calculations were made on these geometries at the MP2/6-31G* level. Frequencies were calculated at the HF/3-21G level and used to calculate zero-point corrections. Tables I and II give the energies of intermediates and transition states calculated at various levels in this investigation. The energy of $C(^1D)$ was estimated as the calculated (UMP2/6-31G* with spin contamination projection[7]) energy of $C(^3P)$ plus the experimental singlet-triplet separation of 30 kcal/mol, a procedure that has worked well in the past.[8-10] The lowest energy pathway for singlet carbon and **1** is assumed to lead to the closed shell solution for complex **3**, between C and **1**, a situation that has applied to the reactions of C with other substrates.[8-10]

(1) Skell, P. S.; Klabunde, K. J.; Plonka, J. H.; Roberts, J. S.; Williams-Smith, D. L. *J. Am. Chem. Soc.* **1973**, *95*, 1547-1552.
(2) For recent reviews of carbon atom chemistry see: (a) Mackay, C. In *Carbenes*; Moss, R. A., Jones, M., Jr., Eds.; Wiley-Interscience: New York, 1975; pp 1-42. (b) Shevlin, P. B. In *Reactive Intermediates*; Abramovitch, R. A., Ed.; Plenum Press: New York, 1980; pp 1-36. (c) Skell, P. S.; Havel, J.; McGlinchey, M. J. *Acc. Chem. Res.* **1973**, *6*, 97-105.
(3) Dervan, P. B.; Dougherty, D. A. In *Diradicals*; Borden, W. T., Ed.; Wiley-Interscience: New York, 1982; pp 107-122.
(4) Forbus, T. R.; Birdsong, P. A.; Shevlin, P. B. *J. Am. Chem. Soc.* **1978**, *100*, 6425-6428.
(5) Binkley, J. A.; Frisch, M.; Raghavachari, K.; Fluder, E.; Seeger, R.; Pople, J. GAUSSIAN 82: Carnegie-Mellon University: Pittsburgh.
(6) Frisch, M. J.; Binkley, J. S.; Schlegel, H. B.; Raghavachari, K.; Melius, C. F.; Martin, R. L.; Stewart, J. J. P.; Bobrowicz, F. W.; Rohlfing, C. M.; Kahn, L. R.; Defrees, D. J.; Seeger, R.; Whiteside, R. A.; Fox, D. J.; Fleuder, E. M.; Pople, J. A. GAUSSIAN 86: Carnegie-Mellon Quantum Chemistry Publishing Unit: Carnegie-Mellon University, Pittsburgh.
(7) Schlegel, H. B. *J. Chem. Phys.* **1986**, *84*, 4530-4534.
(8) Ahmed, S. N.; McKee, M. L.; Shevlin, P. B. *J. Am. Chem. Soc.* **1983**, *105*, 3942-3947.
(9) McKee, M. L.; Shevlin, P. B. *J. Am. Chem. Soc.* **1985**, *107*, 5191-5198.
(10) McPherson, D. W.; McKee, M. L.; Shevlin, P. B. *J. Am. Chem. Soc.* **1985**, *107*, 6493-6495.

0002-7863/90/1512-3374$02.50/0